

# The two dimensional Antiferromagnetic Heisenberg model with next nearest neighbour Ising exchange

J. Hove and A. Sudb  
NTNU  
7491 Trondheim

(Dated: February 8, 2020)

We have studied the  $S = 1/2$  antiferromagnetic Heisenberg model in two dimensions, with an additional Ising next-nearest neighbour interaction. The next-nearest neighbour Ising interaction breaks the isotropy in spin space, for a ferromagnetic next-nearest neighbour interaction the system will order antiferromagnetically along the  $z$  axis. Antiferromagnetic next-nearest neighbour interactions will lead to frustration, and the system responds with tipping the spins down in the  $xy$  plane. For large next nearest neighbour coupling the system will order in a striped phase along the  $z$  axis, this phase is reached through a first order transition. We also consider the case of frustration through disorder on diagonal bonds, and find that any amount of diagonal bond will tilt the magnetization away from the  $z$  axis.

PACS numbers: 75.10.Jm, 75.10.Nr, 75.40.Mg, 75.40.Cx

## I. INTRODUCTION

The groundstate of the antiferromagnetic Heisenberg model is macroscopically degenerate, this makes it particularly sensitive to additional interactions, which might induce transitions to different states[1]. In a seminal paper the concept of fractionalized order, was set forth by Senthil et al. [2] The generic starting point of this analysis is the two dimensional antiferromagnetic Heisenberg model

$$H = J \sum_{\langle i,j \rangle} S_i \cdot S_j + \dots ; \quad (1)$$

where the ellipsis represent additional short range interactions, governed by a coupling  $g$ . For  $g = 0$  the groundstate is the antiferromagnetic Néel state, by tuning  $g$  the system can supposedly be driven through a continuous quantum phase transition to a state with a different type of order. According to the Landau-Ginzburg-Wilson (LGW) paradigm for phase transitions, an order-order transition must either be first order, or go via an intermediate disordered state. Since the scenario envisaged by Senthil et al., a continuous order-order transition, breaks with this paradigm, the term "deconfinement criticality" was coined to describe these transitions.

The only microscopic model considered in some detail in the context of deconfinement criticality is a dimer model with two spins in the unit cell[3]. For this particular model the transition between a Néel state and a spin-gapped paramagnet can be shown analytically, and are also confirmed with QMC calculations[4].

For models with only one spin per unit cell, it is more challenging to construct microscopic models, i.e. find

a suitable set of additional interactions in Eq. 1, which give rise to deconfinement criticality. In particular different forms of ring-exchange[5, 6] have been investigated with these questions in mind. Another possibility is to include frustrated interactions. A natural way to frustrate the Heisenberg model is with a next nearest neighbour (nnn) Heisenberg interaction; this is usually called the  $J_1 - J_2$  model. Unfortunately, in this model the geometric frustration gives rise to a sign problem, and the model is really not amenable to a Monte Carlo based approach. Studies of this model have been based on a reweighting technique[7], exact diagonalization[8] and variational methods[9]. The results indicate that Néel order persists for  $g = J_2 = J_1 = 0.40$ , and that a striped order develops for  $g > 0.60$ . Recent results indicate that the transition at  $g = 0.40$  is a weak first-order transition[10].

To avoid the sign problem of the  $J_1 - J_2$  model, we have studied a simplified model where the nnn exchange is only along the  $z$ -components of the spin, i.e. we have considered the model

$$H = J \sum_{\langle i,j \rangle} S_i \cdot S_j + \sum_{\langle\langle i,j \rangle\rangle} S_i^z S_j^z : \quad (2)$$

For  $g > 0$  the second term in Eq. 16 favors antiparallel spins on nnn bonds, this is in competition with the antiferromagnetic ordering and will inevitably lead to frustration, which will reduce the antiferromagnetic ordering.

The Heisenberg model is isotropic in spin space, whereas the additional next-nearest neighbour interaction in Eq. 2 explicitly breaks this symmetry. Apart from the Heisenberg point at  $g = 0$  we expect three different phases as  $g$  is varied: For  $g < 0$  the system is not frustrated, and the additional next-nearest neighbour will only serve to increase the antiferromagnetic ordering. Observe however that the next-nearest neighbour interaction has singled out the  $z$  direction in spin space,

Electronic address: hove@ntnu.no

i.e. the model should be in the universality class of the Ising model. For  $J > 0$  the system will be frustrated, for moderate  $J$  we expect that the system will avoid the frustration by tipping the spins down in the xy plane, i.e. we will effectively get an antiferromagnetic O(2) model. For larger values of  $J$  the next-nearest neighbour interaction will dominate, in which case the spins will again point along the z axis, and order in one of the striped states illustrated in Fig. 1. In a paper by Roscilde et al.[11] they have studied an antiferromagnetic Heisenberg model with an additional anisotropic next-nearest neighbour exchange, they report Monte Carlo results in the limit of zero transverse nnn interactions; i.e. Eq. 2.

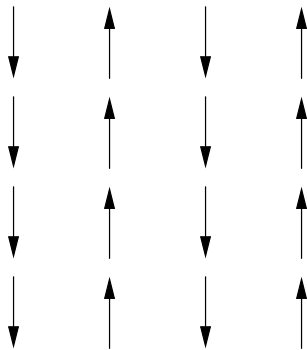


FIG. 1: One classical large configuration.

The  $S = 1/2$  spin models can be exactly mapped to a hardcore boson model, where e.g. spin up represents a particle and spin down a vacancy. Hebert et al.[12, 13] have studied a model very similar to Eq. 16 in the language of hardcore bosons. We essentially reproduce the results of Refs. 11, 12, 13. In addition we have considered the effect of ferromagnetic next-nearest neighbour interactions, and also of next-nearest neighbour bond impurities.

## II. SIMULATIONS

The properties of Eq. 16 have been studied with Quantum Monte Carlo (QMC) simulations. We have used the Stochastic Series Expansion (SSE) [14, 15] method. In the SSE method the Hamiltonian operator is written as a sum of bond operators

$$H = \sum_b (H_{d,b} + H_{od,b}) : \quad (3)$$

The sum in Eq. 3 is over all the bonds in the lattice,  $H_{d,b}$  is an operator working on bond  $b$ , which is diagonal in the basis chosen to represent the spin space, and  $H_{od,b}$  is an off-diagonal operator. For spin models with z axis magnetization as basis, the operator  $H_{d,b}$  will be

$$H_{d,b} = JS_{i(b)}^z S_{j(b)}^z : \quad (4)$$

where  $i(b)$  and  $j(b)$  are the two sites connected by bond  $b$ .  $H_{od,b}$  is an off-diagonal operator, and in the case of spin models we will have  $H_{od,b}$  given by

$$H_{od,b} = \frac{1}{2} S_{i(b)}^+ S_{j(b)}^- + S_{i(b)}^- S_{j(b)}^+ : \quad (5)$$

Observe that for the actual simulations the operators  $H_{d,b}$  are scaled and shifted [15] to ensure

$$H_{d,b} j''#i = j''#i \quad H_{d,b} j'''i = 0 : \quad (6)$$

The formal expression for the partition function is then expanded, which yields the following representation:

$$Z(\beta) = \frac{\prod_{i=1}^n (S_n)^*}{n!} \sum_i Y_i H_i : \quad (7)$$

Here  $S_n$  is a sequence of  $n$  pairs, each pair consisting of a variable denoting operator type and a bond index, i.e.

$$S_n = \underbrace{\{a_1; b_1\}}_{1}; \{a_2; b_2\}; \dots; \{a_n; b_n\} : \quad (8)$$

The variable  $a_i$  in Eq. 8 denotes type of operator and can be either diagonal or off-diagonal. The SSE method then consists of doing importance sampling in the combined space  $\{f, g\}^n S_n$ . The actual updates are of two different types. The diagonal updates insert or remove a diagonal operator  $H_{d,b}$ , thereby changing the expansion order  $n! \rightarrow n-1$ . The off-diagonal operators change operator types  $H_{d,b} \leftrightarrow H_{od,b}$  and flip the corresponding spins, this must be done in a way which ensures periodicity in the direction, i.e.  $j(0)i = j(n)i$ . For the off-diagonal updates the advent of loop updates [16] have significantly improved the performance of SSE [17, 18] simulations.

For the ordinary  $S = 1/2$  Heisenberg model SSE simulations with operator loop update is particularly simple, to include the next-nearest neighbour interactions we must modify the algorithm slightly. For the diagonal updates we must include the extra factor in the weight calculation for the nnn bonds, but apart from that the introduction of next-nearest neighbour bonds leave the algorithm unchanged. For the operator loop the next-nearest neighbour interaction have a more profound effect. These interactions are only diagonal, i.e. the incoming and outgoing spin states must be equal. Furthermore, the next-nearest neighbour bonds can only connect nonparallel ( $J > 0$ ) spins. The result of this is that the next nearest neighbour bonds "freeze" a substantial part of the spin configuration, and only those spins/operators not directly linked to a next-nearest neighbour bond are amenable for operator loop update, this is illustrated in Fig. 2. Clearly this freezing affects the performance of the simulations in a negative way, in particular for intermediate values of  $\beta$ .

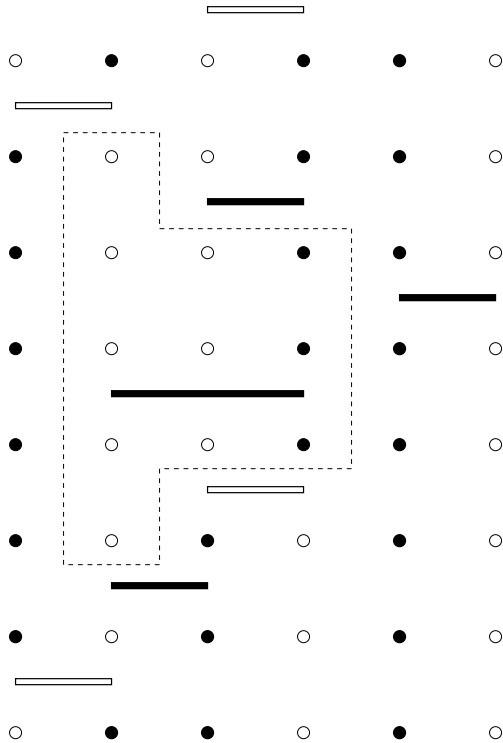


FIG. 2: A chain of six spins, depicted with an operator sequence of length  $n = 8$  in the  $z$  direction. The filled bars denote diagonal interactions  $S_i^z S_j^z$  and the open bars are  $\pm$  operators  $S_i^+ S_j^- + S_i^- S_j^+$ . The dashed region shows spins/p-slices which have been frozen by the next-nearest neighbour bond in the middle.

### III. OBSERVABLES

To differentiate between the different types of order in the model, we have studied the structure factor

$$S(Q) = \frac{1}{N} \sum_{r=1}^N \langle S^z(r) S^z(r+Q) \rangle; \quad (9)$$

for  $Q = (0, 0)$  and  $Q = (\pi, \pi)$ . An estimator of  $S(Q)$  taking all the intermediate SSE states into account can be found in [15]. For the remaining part of the text we will make frequent use of the terms staggered and striped magnetization, these quantities are defined as

$$M_z^{(0,0)} = \frac{1}{N} \overline{3S(0,0)} \quad (10)$$

$$M_z^{(\pi, \pi)} = \frac{1}{N} \overline{S(\pi, \pi) + S(0, \pi)}; \quad (11)$$

The upper index indicates that the magnetization is evaluated along the  $z$  axis, and the lower index is the direction of  $Q$  in the evaluation of Eq. 9, i.e.  $(0, 0)$  for staggered and  $(\pi, \pi)$  for striped magnetization. The factor of three in Eq. 10 is for rotational averaging among the three directions in spin space. When finite symmetry in spin space is explicitly broken, we have nevertheless retained

this factor to get continuous formulas around  $\epsilon = 0$ . In addition to the structure factor we have also measured the internal energy and specific heat

$$E = \frac{\epsilon}{\epsilon} \ln Z = \frac{1}{\epsilon} \ln i \quad (12)$$

$$C_V = \frac{2}{\epsilon^2} \frac{\epsilon^2}{\epsilon^2} \ln Z = \ln^2 i - \ln i^2 - \ln i; \quad (13)$$

and the superuid density. The estimator for the superuid density is [15]

$$s = \frac{3}{4N} \ln N_x^+ N_x^{-2} i + \ln N_y^+ N_y^{-2} i; \quad (14)$$

where  $N^+ = N^-$  is the number of  $S_i^+ S_j^- + S_i^- S_j^+$  operators applied along bonds in the  $z$  direction.

### IV. RESULTS

The main focus of this paper has been to study how the magnetic order is affected by small amounts of additional next-nearest neighbour Ising interaction. To study this we have performed simulations for values in the vicinity of  $\epsilon = 0$ , we have also studied a weakly disordered model which in the clean limit is the Heisenberg point.

For  $\epsilon = 0$  the Mermin-Wagner theorem dictates that there will be no long range order for finite  $T$ , however for  $\epsilon \neq 0$  the isotropy in spin space is broken and the Mermin-Wagner theorem no longer applies a priori. For  $\epsilon < 0$  and large  $T$  the system will effectively break a discrete up-down symmetry along the  $z$  axis, in this case there will be finite  $T$  ordering. For moderate  $\epsilon > 0$  the system will effectively behave as an antiferromagnetic XY model [11]. In this case the Mermin-Wagner theorem applies marginally, with topological order for  $T < T_{\text{KT}}$ . We have briefly determined the phase boundaries of Eq. 16 in the full  $(\epsilon, T)$  plane, however the main focus has been on the ground state properties close to the Heisenberg point.

The remaining part of this section is organized as follows. The properties of the pure system around  $\epsilon = 0$  is presented in section IV A, in section IV B we briefly summarize the properties of the model in the full  $\epsilon, T$  plane and in section IV C we present results of the disordered system.

#### A. The vicinity of $\epsilon = 0$

The Heisenberg model, i.e.  $\epsilon = 0$ , has magnetic order in the groundstate. For  $\epsilon < 0$  this order will be strengthened, whereas  $\epsilon > 0$  will frustrate the groundstate and consequently reduce the magnetic ordering. Fig. 3 shows the staggered magnetization along the  $z$  axis in the vicinity of  $\epsilon = 0$ .

The main features of Fig. 3 are: (i) For  $\epsilon < 0$   $M_z^{(0,0)}$  grows quickly, approaching a fully polarized limit; in this

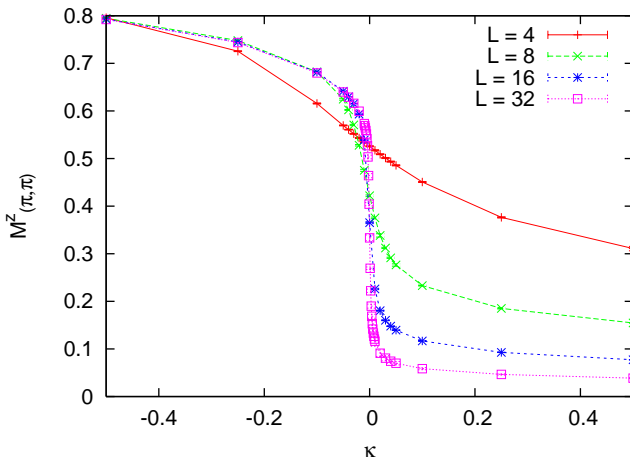


FIG. 3: (Color online) The staggered magnetization along the z axis in the ground state ( $J = 10$ ), as a function of  $\kappa$ .

case the finite size effects are very small. (ii) For  $\kappa > 0$   $M_z(\pi, \pi)$  decays quickly towards a  $L$  dependant value. Figure Fig. 4 shows the finite size behaviour of  $M_z(\pi, \pi)$  in the vicinity of  $\kappa = 0$ . When taking the finite size behaviour in Fig. 4 into account we conclude that any  $\kappa > 0$  is sufficient to push the magnetization away from the z axis. The results for  $\kappa < 0$  indicate that the next-nearest neighbour interaction quickly locks the magnetization into full polarization along the z axis, diminishing the effect of QM spin tipping.

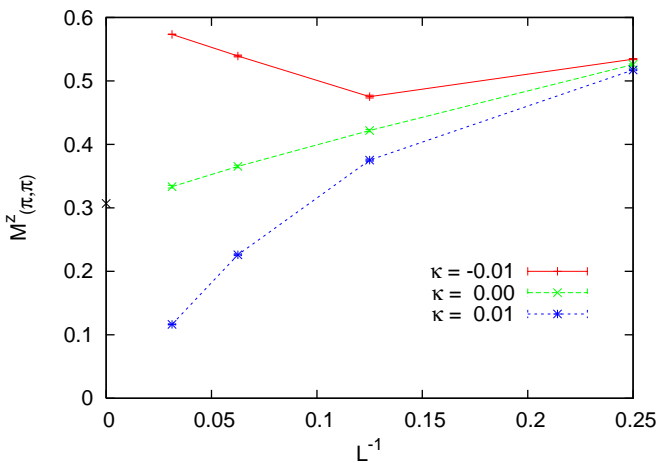


FIG. 4: Finite size scaling of the staggered groundstate magnetization. For  $\kappa = 0$  the  $M_z(\pi, \pi) = 0.307$ , this value is indicated on the ordinate axis[15]. For  $\kappa < 0$   $M_z(\pi, \pi)$  tends to a finite dependant limit and for  $\kappa > 0$   $M_z(\pi, \pi) \neq 0$ .

The magnetic order in the Heisenberg model is a broken continuous symmetry, we therefore have an associated superfluid density. For  $\kappa > 0$  we expect the system to behave effectively as a 0 (2) model, i.e. the superfluid density will persist to  $\kappa > 0$ . On the other hand for  $\kappa < 0$  the resulting system will effectively have a discrete

up-down symmetry, and no associated superfluid density. Figure Fig. 5 shows  $\rho_s$  as a function of  $\kappa$ .

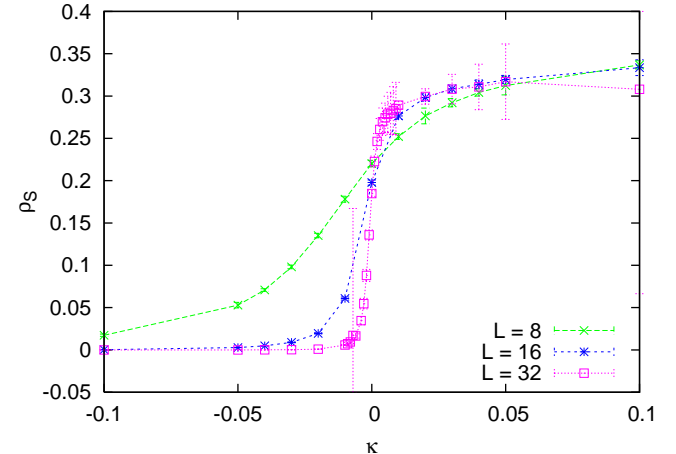


FIG. 5: (Color online) The superfluid density in the ground-state ( $J = 10$ ) as a function of  $\kappa$ .

Fig. 5 closely resembles a mirror of Fig. 3, i.e. for  $\kappa < 0$  the superfluid density quickly vanishes, and for  $\kappa > 0$  it rises to a value greater than the Heisenberg limit. In Fig. 6 we show finite size scaling of  $\rho_s$  in the vicinity of  $\kappa = 0$ , from this figure we conclude that any  $\kappa < 0$  is sufficient to destroy the superfluid properties of the Heisenberg point.

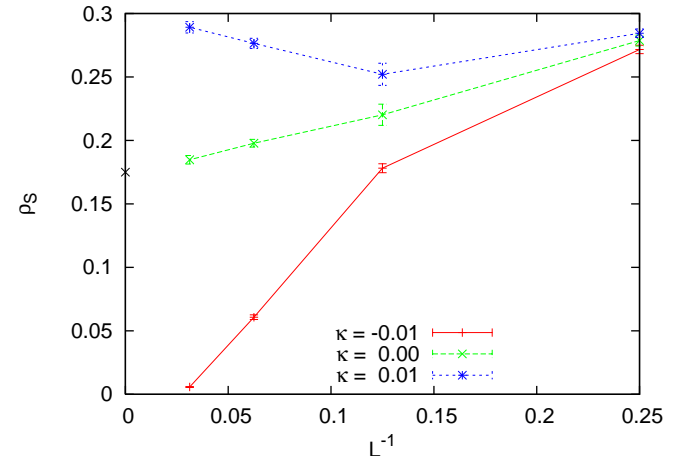


FIG. 6: (Color online) Finite size scaling of the superfluid density, the  $L \rightarrow \infty$  limit  $\rho_s = 0.175$ [15] is indicated on the ordinate axis.

In conclusion what happens when crossing from  $\kappa < 0$  to  $\kappa > 0$  is that the magnetic ordering changes from antiferromagnetic ordering along the z axis for  $\kappa < 0$  to antiferromagnetic ordering in the xy plane for  $\kappa > 0$ . For  $\kappa = 0$  we have antiferromagnetic ordering in an arbitrary direction in spin space. In an analogous manner the superfluid density rises from zero for  $\kappa < 0$ , through an intermediate value at  $\kappa = 0$  and finally a larger value

for  $\kappa > 0$ . In both cases the behaviour across  $\kappa = 0$  is discontinuous, the behaviour is summarized in Fig. 7.

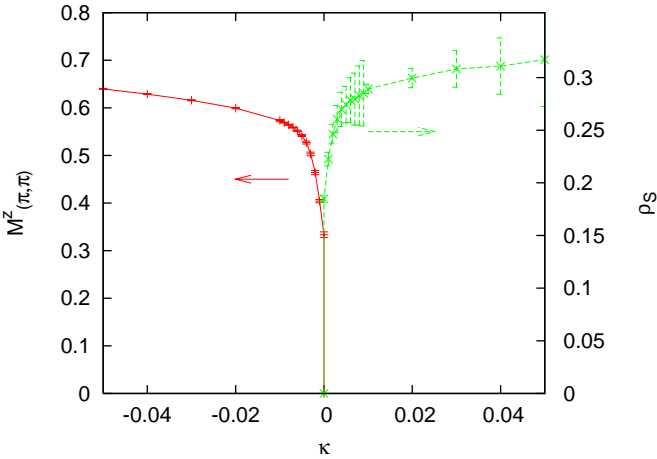


FIG. 7: (Color online) This figure shows the staggered magnetization  $M^z(\pi, \pi)$  and the superfluid density in the immediate vicinity of the Heisenberg point  $\kappa = 0$ . The results are for a  $L = 32$  system at  $\beta = 10$ , for  $\kappa > 0$  ( $\kappa < 0$ )  $M^z(\pi, \pi)$  ( $n_s$ ) has been set to zero, in accordance with the FSS plots in Figs. 4 and 6.

### B. Phase diagram

As discussed in the previous section the groundstate changes character discontinuously when  $\kappa$  is tuned away from zero. In this section we will briefly discuss the properties of the  $\kappa \neq 0$  phases. For  $\kappa = 0$  the Mermin-Wagner theorem rules out the possibility of an ordered state at finite temperature. A finite  $\kappa$  breaks the rotational invariance of the Heisenberg Hamiltonian, and opens up the possibility of an ordered state for finite  $T$ . We have studied the  $T$  dependence of the various ordered phases. The main part of this has already been studied in considerable detail by Rønseide et al. [11] and is included here mainly for completeness.

For large values of  $\kappa$  the next-nearest neighbour interaction will dominate over the nearest neighbour interaction, and the groundstate will again be magnetically ordered along the  $z$  axis, this time of the striped variety. Fig. 8 shows the striped magnetization in the groundstate, as a function of  $\kappa$ . Finite size plots analogous to Fig. 4 (not shown) confirm that the striped magnetization indeed vanishes for  $\kappa < \kappa_c$ , where  $\kappa_c = 1.205$ . The discontinuous jump in Fig. 8 indicates that the transition to a striped phase is first order, and this can be confirmed by histogram analysis of e.g. the striped order parameter [11] or the number of next-nearest neighbour operators. The striped magnetization persists for finite  $T$ , and vanishes through a second order phase transition, the critical temperature is determined from the location of the maximum in the specific heat. This also applies to the Néel ordering for  $\kappa < 0$ .

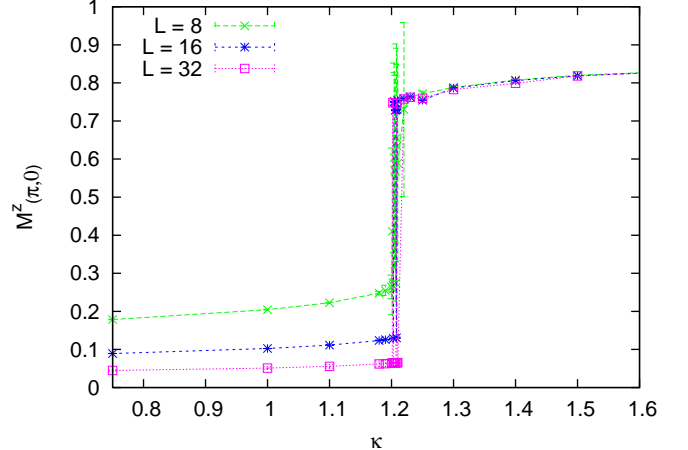


FIG. 8: (Color online) The striped magnetization in the ground state ( $\beta = 10$ ), as a function of  $\kappa$ . There is a first order transition at  $\kappa_c = 1.205$ .

The effect of the next-nearest neighbour interaction in Eq. 2 is to frustrate the model, and to avoid this frustration the spins are tipped from the  $z$  axis and down into the  $xy$  plane. For finite  $T$  there is no long range order in this phase, however there is finite spin stiffness and topological order. This order vanishes in a Berezinskii-Kosterlitz-Thouless transition at  $T_{BKT}$ . The critical temperature  $T_{BKT}$  where superfluid density vanishes is estimated by equating  $s(T)$  with  $2T = 0$ .

Summarizing the results for  $\kappa < 0$ ,  $0 < \kappa < \kappa_c$  and  $\kappa > \kappa_c$  we get phase diagram displayed in Fig. 9. Crossing through  $\kappa = 0$  the properties of the groundstate change discontinuously; for  $\kappa < 0$  we have a broken  $Z_2$  symmetry, right at  $\kappa = 0$  we have a broken  $O(3)$  symmetry and for  $\kappa > 0$  we have a broken  $O(2)$  symmetry. The change of groundstate properties happen discontinuously when crossing  $\kappa = 0$ , i.e. this model is not a candidate for deconfinement criticality. The transition at  $\kappa_c = 1.205$  is first order, and the broken phase has a broken  $Z_2 \times Z_2$  symmetry.

So far the discussion has been based on the Heisenberg model as the starting point, and then perturbing it with additional next-nearest neighbour interactions. Alternatively one can view the model as a nearest and next-nearest neighbour Ising model with an additional interaction which can induce spin flips among nearest neighbours, i.e. an equivalent representation of Eq. 2 is

$$H = J \sum_{\langle i,j \rangle} S_i^z S_j^z + J \sum_{\langle\langle i,j \rangle\rangle} S_i^z S_j^z + \frac{J}{2} \sum_{\langle i,j \rangle} S_i^+ S_j^- + S_i^- S_j^+ : \quad (15)$$

Ignoring the last term we have a pure Ising model, in this case it is diagonal and there are no quantum fluctuations; we will denote this the classical limit. In this particular limit the groundstate is trivial: For  $\kappa < 0.5$  it is a fully polarized antiferromagnet, and for  $\kappa > 0.5$  the groundstate is one of the striped phases illustrated

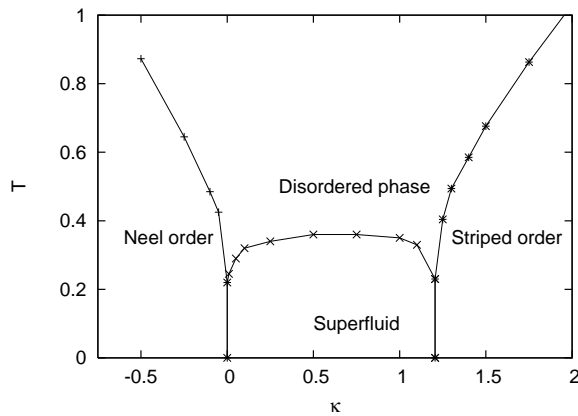


FIG. 9: (Color online) Phase diagram for the model in the  $T$ - $\kappa$  plane. For  $T > \kappa$ , and  $\kappa < 0$  the model has magnetic order, striped and staggered respectively. In the intermediate range values there is no finite  $T$  magnetic order, however there is a superfluid order which persists into the finite  $T$  region. Observe that the line separating topological xy order from the normal phase is determined with considerably less precision than the two other lines.

in Fig. 1. At  $\kappa = 0.5$  where the frustration is maximal the groundstate energy is a singular function of  $\kappa$ . When spin-flip QM fluctuations, i.e. the last term in Eq. 15, are included the transition region is smoothed out, and the groundstate energy is significantly lowered compared to the classical case. Fig. 10 shows the groundstate energy of Eq. 2, along with the classical limit.

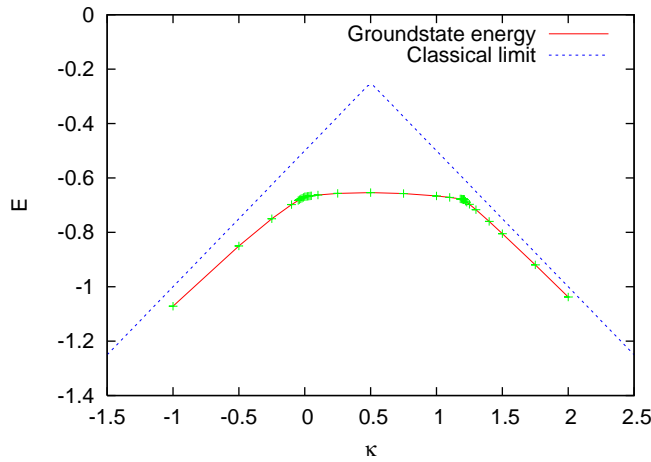


FIG. 10: (Color online) The groundstate energy, and the classical limit. The datapoints are from simulation of  $32 \times 32$  lattice at  $\kappa = 10$ . There is clearly nonanalytic behaviour at  $\kappa = 0$  and  $\kappa = 1.20$ . The groundstate energy has a minimum at  $\kappa = 0.5$ , but apart from that there are no further remnants of the singular feature at  $\kappa = 0.5$ .

### C. Disordered system

As we can see from Fig. 3 any amount of frustration is sufficient to tip the magnetization away from the  $z$  axis. Instead of including a next-nearest neighbour interaction uniformly throughout the lattice, we have started with the ordinary Heisenberg model with only nearest neighbour interactions, and then replaced a fraction  $0 < p < 1$  of the sites with impurity sites. The impurity sites have an additional interaction with their next nearest neighbours. The Hamiltonian for this system is

$$H = J \sum_{\langle i,j \rangle} S_i \cdot S_j + \sum_{\langle\langle i,j \rangle\rangle} i S_i^z S_j^z; \quad (16)$$

where  $i$  is one for impurity sites and zero otherwise. The scenario is illustrated in Fig. 11.

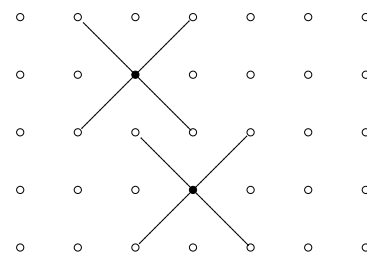


FIG. 11: (Color online) A lattice with two impurities, the additional next-nearest neighbour interactions induced by the impurities are indicated with diagonal lines.

We have kept  $\kappa$  fixed at the value 0.5, and varied  $p$  in the range  $0.000625 \leq p \leq 0.025$ . The results indicate that any finite density of impurities is sufficient to tilt the magnetization away from the  $z$  axis.

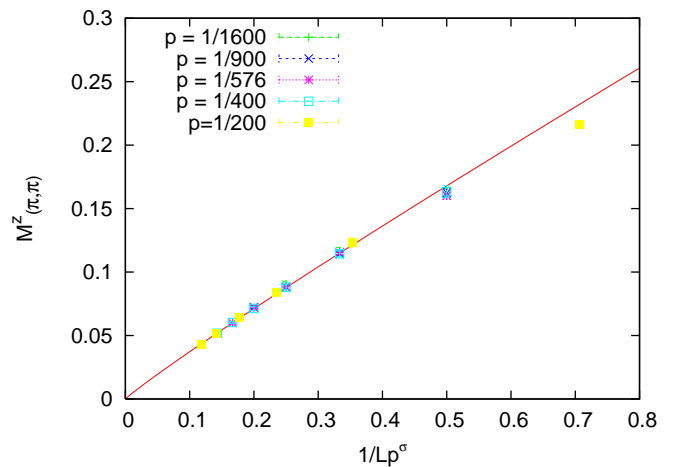


FIG. 12: (Color online) The staggered magnetization as a function of the combination  $(Lp)^a$ , with  $\kappa = 0.5$ . The solid line is a fit with  $a = 0.94$ , added as a guide to the eye.

In Fig. 12 we have plotted  $M_z(\pi, \pi)(x)$ , where  $x$  is the variable  $x = (Lp)^a$ , and  $\kappa = 0.5$ . As we can see, the

data collapse is indeed satisfactory. In the limit  $x \rightarrow 0$  we have the behaviour

$$\lim_{x \rightarrow 0} M^z(0,0)(x)/x = \frac{1}{Lp} \quad : \quad (17)$$

The exponent  $\beta = 0.50$  is determined manually by looking for the best possible data collapse, and  $\beta = 0.94(1)$  is determined from a least squares fit.

## V. CONCLUSION

We have studied the antiferromagnetic Heisenberg model in two dimensions with additional next-nearest neighbour Ising exchange. For any ferromagnetic next-nearest neighbour exchange the magnetization is locked to the  $z$  axis, and the superfluid density vanishes. For any antiferromagnetic next-nearest neighbour exchange the magnetization is tipped down in the  $xy$  plane, and the system effectively behaves as an antiferromagnetic O(2)

model. The tip away from the  $z$  axis can be achieved both with a uniform next-nearest neighbour exchange and with impurities in a disordered system. Because the change of properties happens discontinuously at  $\beta = 0$  this system is not a candidate for exhibiting deconfinement criticality.

## V.I. ACKNOWLEDGEMENT

This work was supported in part by the Research Council of Norway through Grants No. 157798/432 and 158547/431 (NANOMAT) and 167498/V30 (STORFORSK). Bergen Center for Computational Science (BCCS) is acknowledged for computing time.

## Bibliography

---

- [1] A. Cuccoli, T. Roscilde, V. Tognetti, R. Vaia, and P. Verrocchi, *Phys. Rev. B* 67, 104414 (2003).
- [2] T. Senthil, A. Vishwanath, L. Balents, S. Sachdev, and M. P. A. Fisher, *Science* 303, 1490 (2004).
- [3] S. Sachdev, *Quantum magnetism* (Springer, 2004), chap. Quantum phases and phase transitions of Mott insulators.
- [4] M. Matsumoto, C. Yasuda, S. Todo, and H. Takayama, *Phys. Rev. B* 65, 014407 (2001).
- [5] A. W. Sandvik, S. Daul, R. R. P. Singh, and D. J. Scalapino, *Phys. Rev. Lett.* 89, 247201 (2002).
- [6] R. G. Melko, A. W. Sandvik, and D. J. Scalapino, *Phys. Rev. B* 69 (2004).
- [7] T. Nakamura and N. Hatano, *Journal of the Physical Society of Japan* 62, 3062 (1993).
- [8] H. J. Schulz, T. A. L. Ziman, and D. Poilblanc, *J. Physique I* 6, 675 (1996).
- [9] L. Capriotti, F. Becca, A. Parola, and S. Sorella, *Phys. Rev. Lett.* 87, 097201 (2001).
- [10] J. Sirker, Z. Weihong, O. P. Sushkov, and J. O. Rønnow, *cond-mat* (2006).
- [11] T. Roscilde, A. Feiguin, A. L. Chernyshev, S. Liu, and S. Haas, *Phys. Rev. Lett.* 93, 017203 (2004).
- [12] F. Hebert, G. G. Batrouni, R. T. Scalettar, G. Schmid, M. Troyer, and A. D. Orenreich, *Phys. Rev. B* 65, 014513 (2001).
- [13] G. Schmid and M. Troyer, *Phys. Rev. Lett.* 93, 067003 (2004).
- [14] A. W. Sandvik and J. Kurkijärvi, *Phys. Rev. B* 43, 5950 (1991).
- [15] A. W. Sandvik, *Phys. Rev. B* 56, 11678 (1997).
- [16] H. G. Evertz, G. Lana, and M. Martínez, *Phys. Rev. Lett.* 70, 875 (1993).
- [17] A. W. Sandvik, *Phys. Rev. B* 59 (1999).
- [18] O. F. Syljåsen and A. W. Sandvik, *Phys. Rev. E* 66, 046701 (2002).